Uptake and trafficking of fluorescent conjugates of folic acid in intact kidney determined using intravital two-photon microscopy

Ruben M. Sandoval,[1,2] Michael D. Kennedy,[3] Philip S. Low,[3] and Bruce A. Molitoris[1,2]

[1]*Division of Nephrology, Department of Medicine, Indiana University School of Medicine, and The Indiana Center for Biological Microscopy, Indianapolis;* [3]*Department of Chemistry, Purdue University, West Lafayette, Indiana 47907; and* [2]*The Roudebush Veterans Affairs Medical Center, Indianapolis 46202*

Submitted 6 January 2004; accepted in final form 1 April 2004

Sandoval , Ruben M., Michael D. Kennedy, Philip S. Low, and Bruce A. Molitoris. Uptake and trafficking of fluorescent conjugates of folic acid in intact kidney determined using intravital two-photon microscopy. *Am J Physiol Cell Physiol* 287: C517–C526, 2004. First published April 21, 2004; 10.1152/ajpcell.00006.2004.—Intravital two-photon microscopy was used to follow the uptake and trafficking of fluorescent conjugates of folic acid in the rat kidney. Intravenously administered folate-linked dye molecules quickly filled the plasma volume but not cellular components of the blood. Glomerular filtration occurred immediately and binding to proximal tubule cells was seen within seconds. Fluorescence from a pH-insensitive conjugate of folic acid, folate Texas red (FTR), was readily observed on the apical surface of the proximal tubules and in multiple cellular compartments, but little binding or uptake could be detected in any other kidney cells. Fluorescence from a pH-sensitive conjugate of folic acid, folate fluorescein, was seen only on the apical surface of proximal tubule cells, suggesting that internalized folate conjugates are localized to acidic compartments. The majority of the FTR conjugate internalized by proximal tubules accumulated within a lysosomal pool, as determined by colocalization studies. However, portions of FTR were also shown by electron microscopy to undergo transcytosis from apical to basal domains. Additional studies with colchicine, which is known to depolymerize microtubules and interrupt transcytosis, produced a marked reduction in endocytosis of FTR, with accumulation limited to the subapical region of the cell. No evidence of cytosolic release of either folate conjugate was observed, which may represent a key difference from the cytosolic deposition seen in neoplastic cells. Together, these data support the argument that folate conjugates (and, by extrapolation, physiological folate) bind to the apical surface of proximal tubule cells and are transported into and across the cells in endocytic compartments.

proximal tubule cell

THE KIDNEY IS A WELL-CHARACTERIZED MODEL for folate trafficking because it represents the body's final prospect to recapture folate and thereby minimize loss to excretion. Because the mean serum concentration of folate is ~10 ng/ml and the amount of plasma protein binding of folate is too low to prevent filtration through the kidney glomulerus (15, 26, 48), it has been estimated that more than 1 mg/day of folate is filtered through the kidneys (48). Because this value is at least 20 times the measured urinary levels of folate (11), an efficient mechanism must exist for folate reabsorption by the kidneys.

Two folate transport proteins have been identified in kidney tissue: the reduced folate carrier (RFC) and the folate receptor (FR) (27, 33, 49, 51). The RFC is found on the basolateral surface of kidney proximal tubule cells (55), while FRs are found on the apical brush-border membrane (3, 12, 22, 24, 49). Folate retention and transport back into blood vessels is known to be saturable (2), involving rapid uptake followed by slow transcytosis (50). Folate gold particles have been localized within coated pits and coated vesicles (2). FRs also have been colocalized to compartments of the clathrin-coated pit endocytic pathway (2, 3, 9, 10, 14, 22, 25, 32, 34–37, 41, 48, 50, 52). Although these studies are illuminating, investigators have not yet been able to continuously track the intracellular path taken by folic acid after its initial binding to the apical brush border in living animals.

Recent advances in two-photon fluorescence microscopy have sparked an interest in intravital imaging (see references cited in Ref. 13). Briefly, the longer, far-red wavelengths used for double harmonic fluorescence excitation provide deeper optical penetration into biological specimens with less light scatter while illuminating only the sample plane in focus. This also results in markedly reduced phototoxicity when viewing a through-focus volume (13).

In the present studies, we used fluorescein and Texas red conjugates of folate (FF and FTR, respectively) in conjunction with two-photon microscopy to examine the uptake of folic acid into kidney proximal tubules. Our data demonstrate folate binding at the apical surface with subsequent uptake via endocytosis as well as the dynamic movement of FTR into and across the intact kidney.

Electron microscopic studies in which photoconversion techniques were used (17, 39, 45, 53, 54) revealed fusion of these small vesicles with the basolateral membrane domain, documenting transcytosis. Studies in which the microtubule depolymerizing agent colchicine was used revealed reduced apical uptake with no trafficking of endocytic vesicles below the subapical region of proximal tubules. In addition, long after the initial infusion of FTR and clearance from the proximal tubule lumen, staining persisted at the apical surface that was far too intense to be attributed solely to receptor binding. This observation may represent a novel mechanism by which proximal tubule cells sequester and retain folate for subsequent internalization, thereby preventing loss by excretion.

MATERIALS AND METHODS

Fmoc-protected amino acid derivatives, Fmoc-glycine-loaded Wang resin, 2-(1*H*-benzotriazol-1-yl)-1,1,3,3-tetramethyluronium hexafluorophosphate (HBTU), and *N*-hydroxybenzotriazole were pur-

Address for reprint requests and other correspondence: B. A. Molitoris, Division of Nephrology, Department of Medicine, Indiana Univ. School of Medicine, 950 W. Walnut St., R2 Bldg. E202-C, Indianapolis, IN 46202 (E-mail: bmolitor@iupui.edu).

chased from Novabiochem (San Diego, CA). N^{10}-trifluoroacetylpteroic acid was synthesized from folic acid (Sigma, St. Louis, MO) as described previously (31). Synthesis of γ-COOH terminus-linked folate fluorescein was described in a previous report (28). Balb/c mice and folate-deficient chow were purchased from Harlan (Indianapolis, IN). The sources of other chemicals are described in text.

Synthesis of folate conjugates. Standard Fmoc peptide chemistry was used to synthesize a folate peptide linked to Texas red attached to the γ-COOH terminal of folic acid. The sequence Gly-Lys-(γ)Glupteroic acid was constructed by Fmoc chemistry with HBTU and *N*-hydroxybenzotriazole as the activating agents along with diisopropyethylamine as the base and 20% piperidine in dimethylformamide (DMF) for deprotection of the Fmoc groups. Fmoc-protected lysine containing a 4-methyltrityl protecting group on the ε-amine was linked to Fmoc-protected glycine attached to a Wang resin. An α-t-Boc-protected *N*-α-Fmoc glutamic acid was then linked to the peptide to provide a γ-linked conjugate on folate after N^{10}-trifluoroacetylpteroic acid was attached to the peptide. The methoxytrityl protecting group on the ε-amine of lysine was removed with 1% trifluoroacetic acid in dichloromethane to allow attachment of Texas red. Texas red *N*-hydroxysuccinimide (Molecular Probes, Eugene, OR) in DMF was reacted overnight with the peptide and then washed thoroughly from the peptide resin beads. The FTR peptide was then cleaved from the resin with 95% trifluoroacetic acid-2.5% water-2.5% triisopropylsilane solution. Diethyl ether was used to precipitate the product, and the precipitant was collected by centrifugation. The product was then washed twice with diethyl ether and dried under vacuum overnight. The product was then analyzed and confirmed by mass spectroscopic analysis ($[M^-]$ calculated, 1,423; found, 1,422). To remove the N^{10}-trifluoracetyl protecting group, the product was dissolved in 5 ml of water containing 0.5 ml of 10% ammonium hydroxide and stirred for 30 min at room temperature. The product was then precipitated with combined isopropanol and ether, and the precipitant was collected by centrifugation. The product was then added to a G-10 Sephadex gel filtration column (1.5 × 15 cm) with water used as the eluent. The product peaks were collected and lyophilized.

Animal model. Male Sprague-Dawley or Munich-Wistar rats initially weighing between 200 and 250 g were placed on a folate-deficient diet for 2–4 wk before the studies. For some studies, adult male balb/c mice weighing ~20 g were placed on a folate-deficient diet 2–4 wk before imaging. The rats and mice were anesthetized with pentobarbital sodium (55 mg/kg body wt; Besse Scientific, Louisville, KY) (13) before surgery.

Surgical procedures. The anesthetized animal's midsection was shaved completely, and a small, 10- to 15-mm lateral incision was made dorsally. The kidney was gently externalized, and fluorescent probes were infused by one of three methods: *1*) a femoral venous line inserted into the left leg, *2*) a butterfly catheter inserted into the tail vein, or *3*) intraperitoneal (IP) injection. Regardless of delivery method, the eventual intracellular localization was identical; however, IP injection provided a more protracted delivery of the probes with greater clearance times, because absorption into the bloodstream was significantly prolonged.

Fluorescent probes. Fluorescent probes were injected in a bolus with normal saline used as a carrier as described in *Surgical procedures* in a total combined volume not exceeding 1 ml. In rat studies, ~600 μg (200 μg for mice) of the dye Hoechst 33342 (Molecular Probes) was used for nuclear staining (13) and was injected 5–10 min before FTR injection to allow time for incorporation. Approximately 2 mg of a small, 3,000 mol wt fluorescent dextran conjugated to the pH-insensitive dye Alexa 488 (Molecular Probes) was sometimes injected to localize the lysosomes (13). A 10,000 mol wt rhodamine dextran and a 500,000 mol wt amino dextran conjugated to rhodamine (Molecular Probes) were used to label the proximal tubules and microvasculature, respectively, in the FF studies. In rat studies, ~200 μg (80 μg for mice) of FTR or FF were injected.

Lysosomal localization, colchicine treatment, and nonfluorescent folate competition experiments. The 3,000 mol wt Alexa 488 dextran mentioned above was injected ~1.5 h before FTR infusion to fluorescently label the lysosomes (13). This was done to ensure that the early endosomal compartment would be free of all traces of the dextran before FTR was introduced. To further characterize the abundance of FTR localization to the apical brush border in proximal tubule cells, rats were first labeled with dextran as described and then infused with a 10-fold excess of folic acid (Sigma) in normal saline, pH 7.0, followed by FTR infusion 10 min later. For colchicine treatment studies, 3.2 mg/kg body wt of colchicine was injected intraperitoneally into balb/c mice 12 h before imaging (44).

Microscopy. A Bio-Rad MRC-1024 two-photon laser scanning microscope (Hercules, CA) mounted on a Nikon Diaphot inverted stage platform (Fryer, Huntley, IL) with a Ti:Sapphire laser (Spectra-Physics, Franklin, MA) was used. Acquisition parameters and placement of the rat on the microscope stage were performed as previously described (13). All images were collected with the use of a ×60 water-immersion objective with a numerical aperture of 1.2. A wavelength of 800 nm was used to excite the mixture of fluorescent probes.

Image processing and volume rendering. Images were processed, and three-dimensional projections were generated from through-focus data sets using Voxx rendering software (a proprietary software program developed at the Indiana Center for Biological Microscopy facility, available as freeware) or Metamorph (Universal Imaging, West Chester, PA) as previously described (13).

Electron microscopy. Approximately 1 h after FTR infusion, the kidney was excised and small pieces were cut and fixed in 4% freshly thawed paraformaldehyde in PBS overnight. The specimens were then washed briefly in PBS, and 100-μm-thick vibratome sections were cut from the outer cortex. The thin sections were photoconverted and processed routinely for electron microscopy as previously described (46, 53).

RESULTS

Initial studies were conducted to determine the trafficking characteristics of fluorescent folate conjugates within the functioning kidney. Several characteristics were documented in previous studies (13) that detailed the specifics of renal morphology visualized in this manner. Before folate dye conjugate infusion, the nuclear dye Hoechst 33342 was administered to visualize the nuclei of all cell types and to facilitate the identification of renal landmarks (cyan blue fluorescence in all color micrographs). The nuclei of distal tubules stain brighter than those of proximal tubules, and those of endothelial cells stain less intensely and are elongated. Injection of FF resulted in green fluorescence on the apical side of the proximal tubule cells, with no noticeable fluorescence seen in the interior of the cell even after 28 and 43 min of uptake (Fig. 1, *A* and *B*, respectively). Uptake into low-pH endocytic vesicles most likely accounted for the lack of intracellular fluorescence, because folate is known to be endocytosed and the fluorescence intensity of fluorescein decreases in a low-pH environment (2, 3, 22).

Confirmation that folate conjugates are taken into low-pH endosomes in the cell interior was found after observing uptake of pH-insensitive FTR into proximal tubule cells (Fig. 2). A time series was acquired during the initial infusion of FTR and made into a movie (Movie 1). Please refer to the Supplementary Material[1] for this article (published online at the *American*

---

[1] Supplementary Material to this article (Movies 1 and 2) is available online at http://ajpcell.physiology.org/cgi/content/full/00006.2004/DC1.
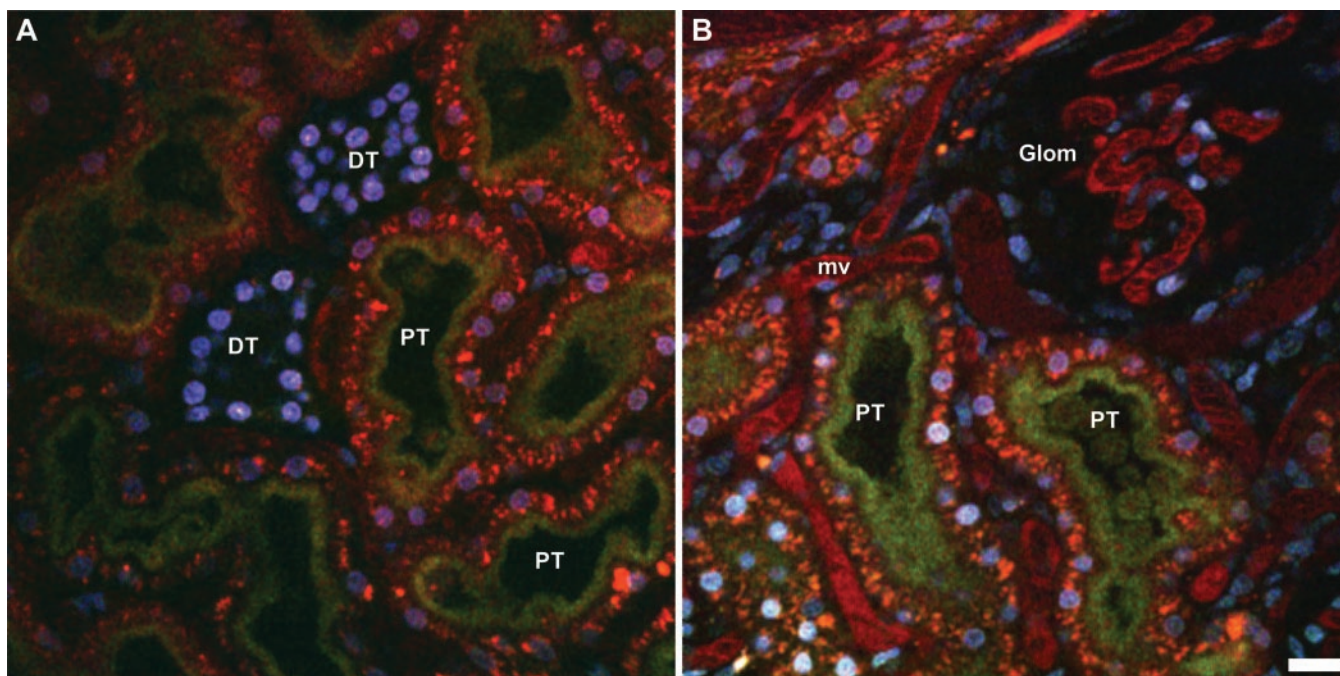
Fig. 1. Multicolor 2-photon micrographs of folate fluorescein (FF) infusion in the rat kidney of a Munich-Wistar rat. The nuclei (blue) were labeled with Hoechst 33342, and small- and large-molecular-weight rhodamine-labeled dextran were used to localize the endocytic compartment of proximal tubules (PT) and the renal microvasculature (mv), respectively, before FF infusion. FF fluorescence is seen on the apical brush-border membrane even 28 (*A*) and 43 (*B*) min postinjection. At no time during the study did the appearance of small FF-containing endocytic vesicles occur, as was seen in the subsequent studies in which folate Texas red (FTR) was used. Glom, glomerulus; DT, distal tubules. Bar = ~10 μm.

Journal of Physiology-Cell Physiology web site) to view the movie. The 1st and 16th frames of this data set are shown in Fig. 2, *A* and *B*, respectively. First, a punctate orange autofluorescence emanating from the proximal tubules before FTR infusion is seen. This autofluorescence is associated with the lysosomes of proximal but not distal tubules (Fig. 2*A*). The microvasculature appears as a labyrinth around the tubules, devoid of any intrinsic fluorescence. Approximately 2–3 s after FTR infusion is initiated, the red fluorescent probe quickly fills the plasma component of the blood and is seen throughout the microvasculature (Fig. 2*B*). The circulating red blood cells appear as dark, oblong shadows as they exclude the fluorescent probe (Fig. 2*B*, arrowheads). The small size of the probe (<1,500 daltons) facilitates migration out of the blood vessels and into the peritubular space. After 3–4 min, the vast majority of FTR is filtered from the blood and cleared from the peritubular space. Within as little as 3–4 min, evidence of endosomes is seen at the apical region of proximal tubule cells (Fig. 2*C*, arrows). This becomes more pronounced with time (Fig. 2, *D–F*). At the apical surface of proximal tubules, a delineation between the microvilli and the subapical region is apparent (Fig. 2, *C* and *D*, arrowheads). A frame (Fig. 2*E*) taken from a time series shows discrete vesicles at the basal side (arrows). These individual vesicles can be seen moving throughout the cells in the movie generated from this time point (Movie 2).

Through-focus data sets for the different tubule segments, whether proximal or distal, show vastly different accumulation patterns. Three-dimensional reconstruction images obtained at early and later time points for proximal tubules show punctate structures distributed throughout the cells (Fig. 3, *A* and *C*). Early in the process, the larger endogenous autofluorescent structures exhibit their characteristic orange profile (Fig. 3*A*). As accumulation continues, the color in these structures shifts from orange to red (Fig. 3*C*). Distal tubules failed to internalize significant quantities of FTR (Fig. 3, *B* and *D*). Occasionally, some faint endocytic structures were seen (Fig. 3, *B* and *D*, arrowheads). In these tubules, the dye appears to have accumulated passively within the luminal space (Fig. 3, *B* and *D*) as a consequence of water reabsorption. Thus, as the segment progressed and water reabsorption increased, the intensity of FTR became brighter in the lumen as the relative FTR concentration increased. The nuclei of distal tubules (Fig. 3, *B* and *D*), which are the only fluorescent cellular structures, surround the bright luminal volume.

Several studies of the endocytic pathway of folate receptors in which kidney cells, MA104, as well as other cell lines were used have indicated that caveolae are involved in folate receptor endocytosis (1, 8, 42, 43). Other studies have shown that folate receptors are localized to clathrin-coated-pits and vesicles (2, 3, 22). To evaluate the endocytosis pathway of folate in living kidney proximal tubules, we examined FTR uptake after colchicine infusion, as described in METHODS. As shown in Fig. 4, FTR accumulated in endosomes of untreated mice (*A, A′, B,* and *B′*), and produced a staining pattern similar to that seen in rats. In the enlarged panels (*A′* and *B′*), endocytic vesicles were observed to traffic well within the interior of proximal tubule cells, toward the basal membrane. Pretreatment with colchicine (*C, C′, D,* and *D′*) markedly reduced uptake, and accumulation was confined to the subapical region of proximal tubules. No evidence of FTR-containing vesicles near the basal membranes was observed.
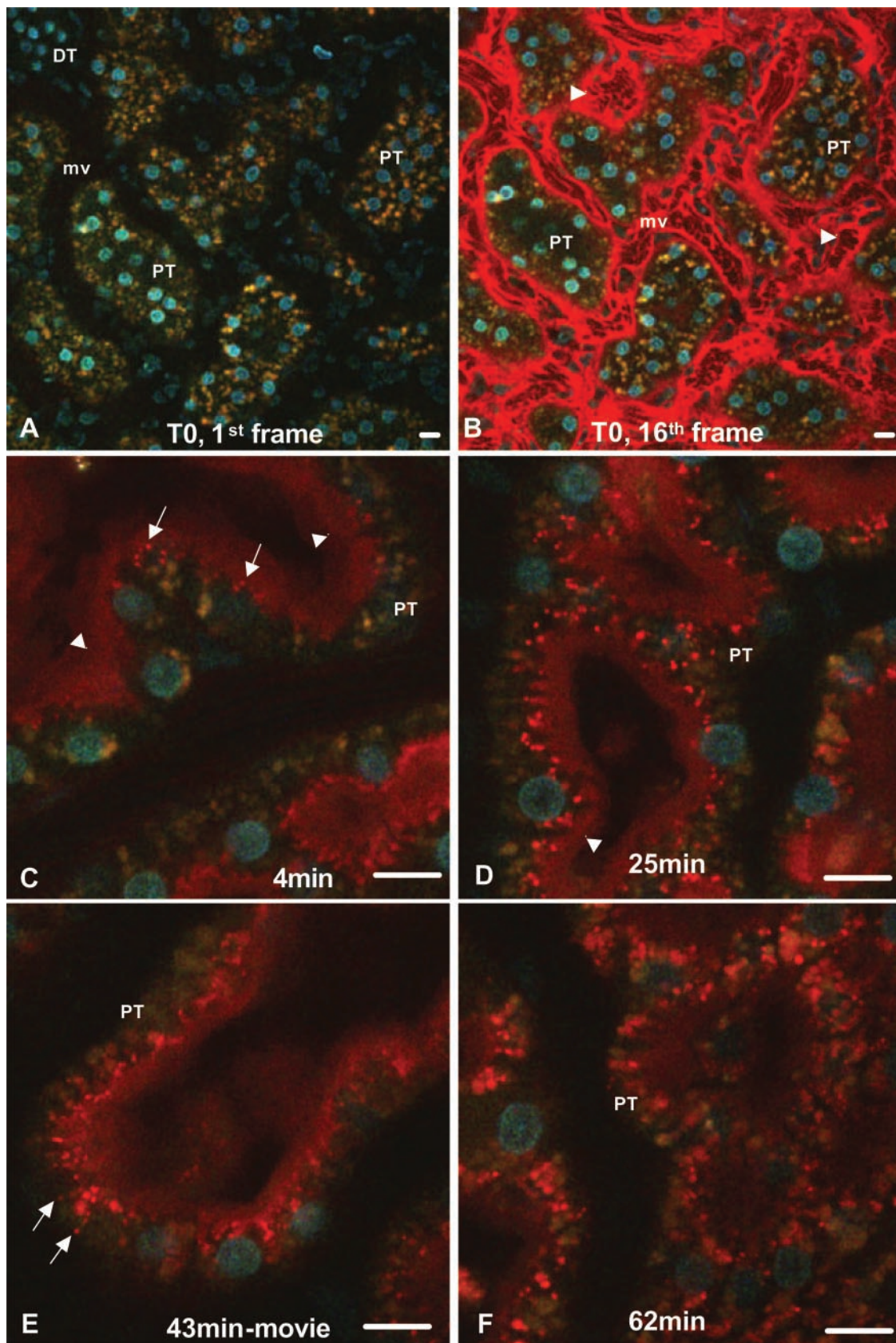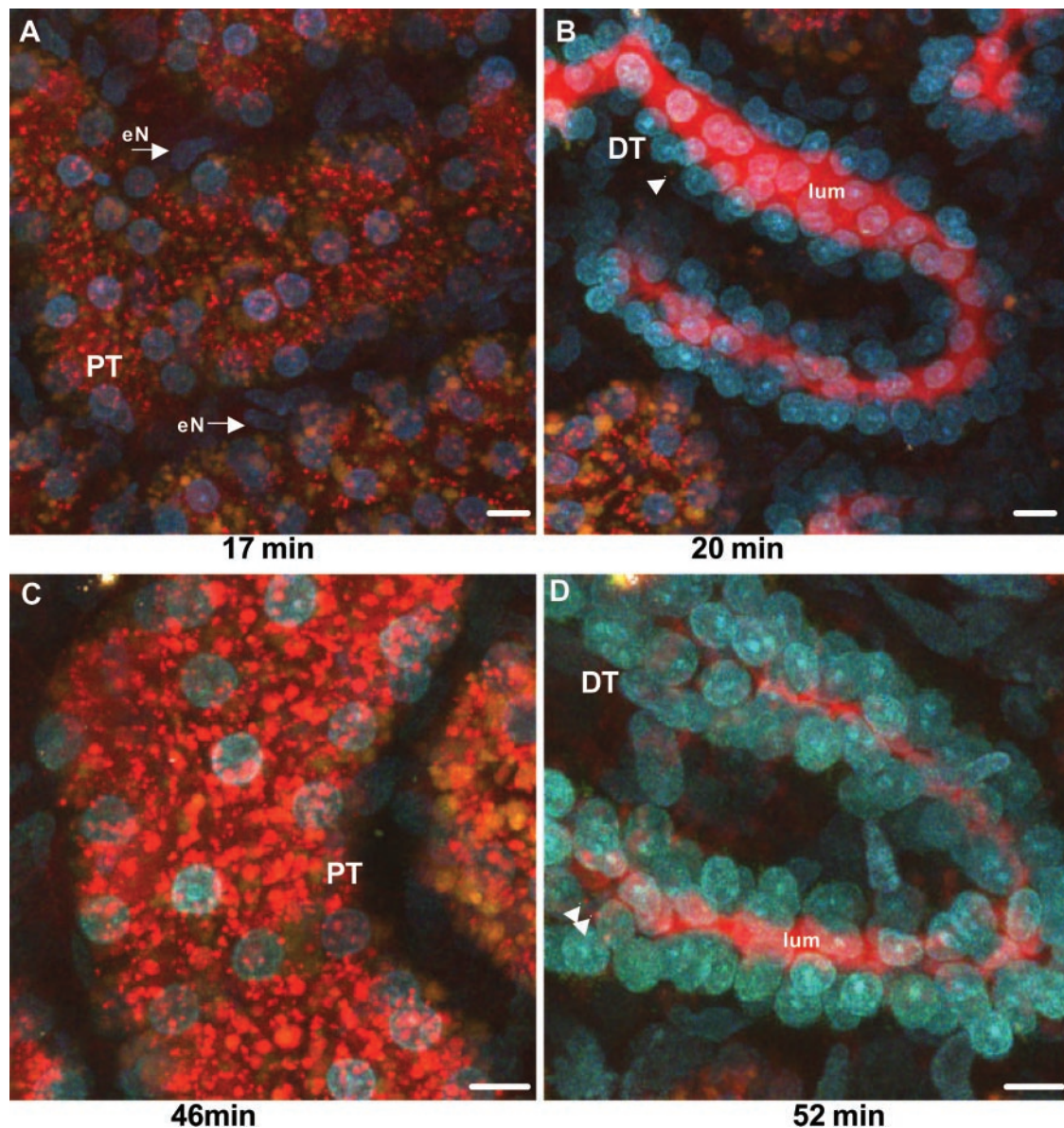
Fig. 3. Three-dimensional micrographs showing different FTR accumulation patterns between proximal and distal tubules. In proximal tubules, the number and intensity of small endocytic vesicles seen at earlier time points (*A*) are subsequently enhanced (*C*). Here, fusion of FTR appears to occur with the autofluorescent lysosomal compartment as a shift in the spectrum from orange to red occurs. In distal tubules (*B* and *D*), accumulation of the probe is limited to the lumen (lum), with evidence of internalization via endocytosis (*B* and *D*, arrowhead) being very rare. Even 1 h postinfusion, the probe is still retained in the lumen. eN, endothelial cell nuclei. Bars = ~10 μm.

Having gathered preliminary data to suggest both lysosomal accumulation of FTR and transcytosis from the apical to the basal membrane, we undertook colocalization studies. Briefly, rats were exposed to a low-molecular-weight, pH-insensitive, green-emitting fluorescent dextran to label the lysosomes ~1.5 h before FTR infusion. As expected, the majority of the inherent orange autofluorescence was replaced with green-yellow fluorescence associated with the dextran (Fig. 5). Over

Fig. 2. Multicolor 2-photon micrographs of FTR infusion in the rat kidney. The 1st (*A*) and 16th (*B*) frames of the initial stages of a movie showing FTR infusion may be viewed in Movie 1 (Supplementary Material for this article may be viewed online). Hoechst 33342 was administered before FTR infusion to identify different areas within the kidney. Most prominently, the proximal tubules contain an inherent punctate, orange autofluorescence that is absent in distal tubules. The microvasculature appears empty at the start (*A*), but the plasma volume is quickly filled a few seconds after infusion (*B*). Circulating blood cells (*B*, arrowheads) appear as oblong shadows because they exclude the fluorescent probe. Early endocytic vesicles (*C*, arrows) are seen within as little as 4 min. Also, delineation between microvilli and the subapical region can be seen in proximal tubule cells throughout the study (arrowheads). At subsequent time points (*D–F*), greater evidence of endocytic accumulation is present, with formation of large FTR-containing aggregates. A frame (*E*) from a time series (Movie 2) shows movement of endocytic vesicles (arrows) throughout the proximal tubule cells. Bars = ~10 μm.
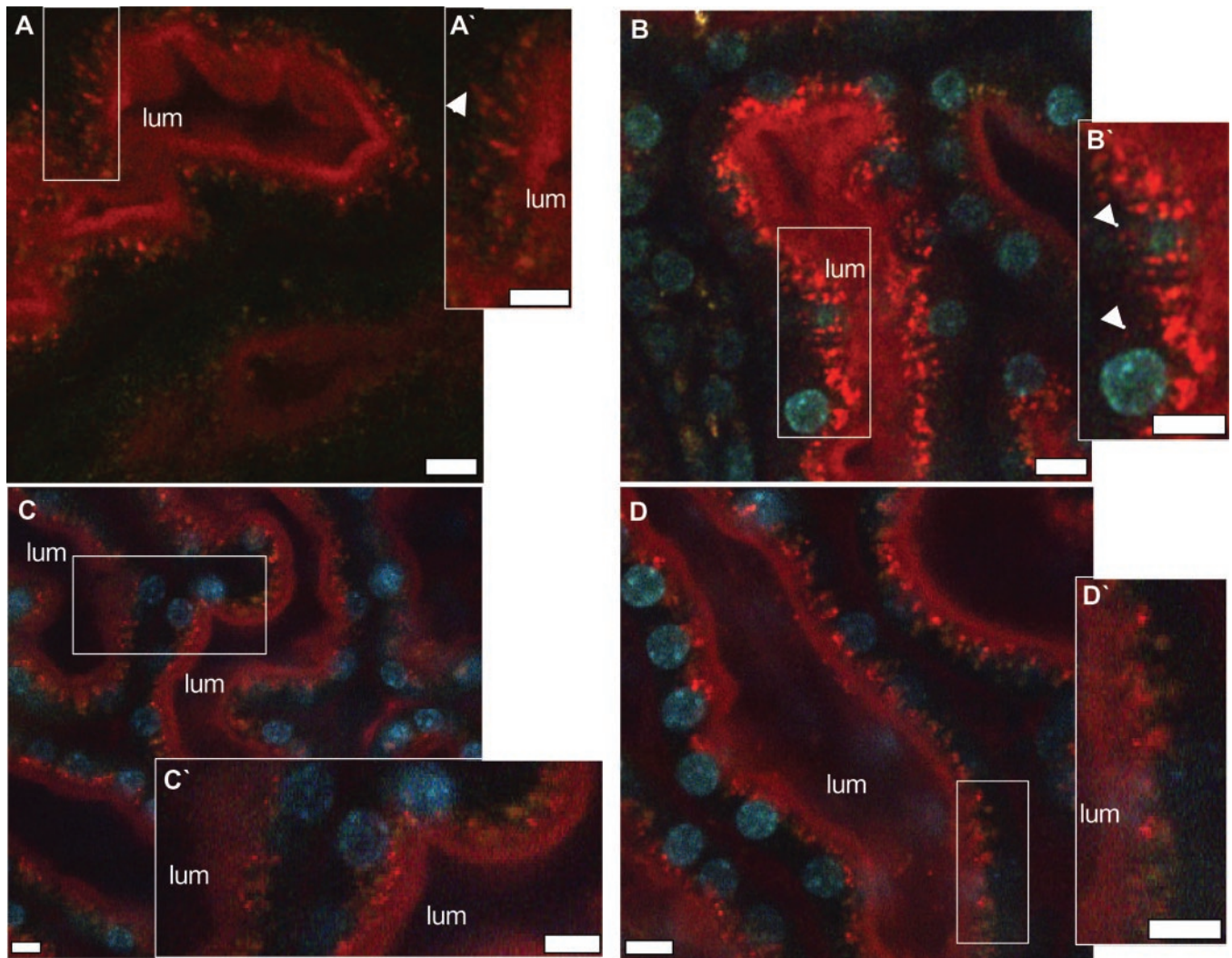
Fig. 4. Mice were preinjected intraperitoneally with 3.2 mg/kg body wt of colchicine 12 h before imaging with FTR. Micrographs from control mice at 30 (*A, A′*) and 70 (*B, B′*) min postinjection exhibited staining patterns similar to those seen in rats. In *A′* and *B′*, there is evidence of small FTR-containing vesicles near the basal surface. Colchicine-treated mice that underwent FTR injection exhibited a reduction in the number of endocytic vesicles at the apical surface 40 (*C* and *C′*) and 60 (*D* and *D′*) min postinjection. None of the vesicles seen in the colchicine-treated mice were localized near the basolateral surface (*C′* and *D′*). Bars = ~10 μm. Images in *A* and *A′* were obtained before infusion of Hoechst 33342 and therefore show no nuclear labeling.

time, the green-yellow fluorescence became more reddish-yellow as FTR accumulated within the same lysosomes (Fig. 5*B*). Even after 1 h had elapsed, small, discrete vesicles containing FTR, but not dextran, could be seen at both the apical (arrows) and basal (arrowheads) portions of the cells (Fig. 5*B*). Exposure to a 10-fold excess of folate before FTR infusion did not totally inhibit apical binding (Fig. 5, *C* and *D*, asterisks) or internalization in proximal tubule cells, although both appeared to be decreased (Fig. 5, *C* and *D*). Even after 1 h had elapsed in the excess folate-treated rats, apical binding at the microvilli was still evident (Fig. 5*D*, arrows).

After a small vesicular staining pattern was observed near the basal membranes, it became necessary to visualize these structures at the electron microscopic level to determine if transcytosis occurred. Photoconversion of Texas red in the presence of diaminobenzadine produces an electron-dense precipitant that becomes denser upon reaction with osmium tetroxide (46, 53). The reaction product was readily seen in vesicular structures throughout the cytosol, localized around their inner membrane (Fig. 6, *A* and *B*, arrowheads). Adjacent to the basolateral membrane, smaller vesicles, some less than 1 μm in diameter, contained reaction product (Fig. 6, arrowheads). The content of vesicles located well within the cytosol appeared more opaque because of the proteinaceous content (Fig. 6, asterisks). Conversely, the smaller punctate vesicles adjacent to the apical and basal membranes are less opaque (Fig. 6, *A* and *B*, plus signs), and they match the density of the extracellular space beyond the membrane, indicating a direct communication.

DISCUSSION

Folic acid is an essential vitamin for cell division and cellular metabolism. Dietary deficiencies in folic acid have been linked to anemia (16, 20, 23), neurological disorders (4, 5, 38, 56), amblyopia (4, 5, 18, 19, 29, 38, 56), neural tube
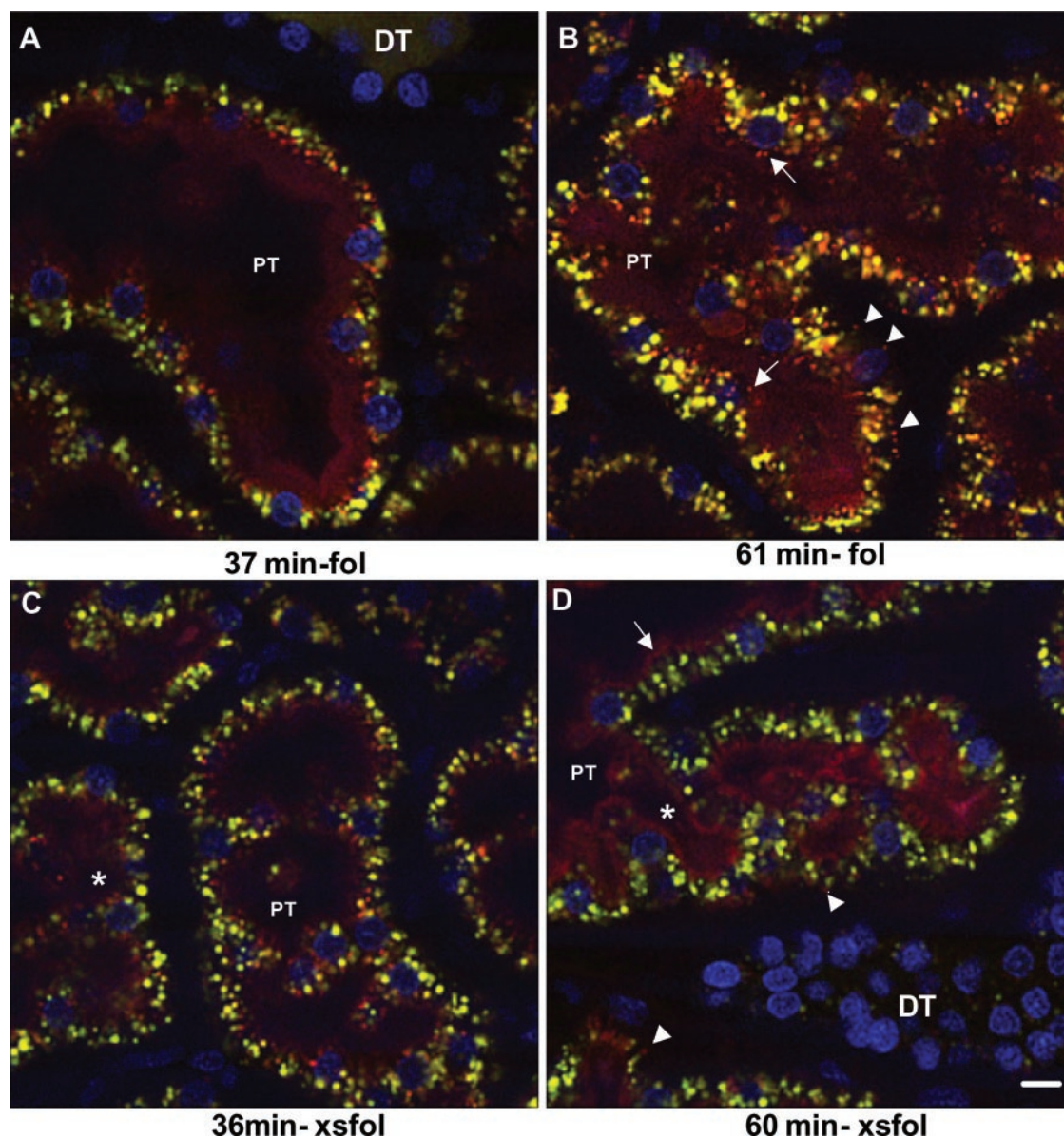
Fig. 5. Rats were administered a low-molecular-weight, pH-insensitive dextran to localize the lysosomes 1.5 h before FTR infusion. The shift from orange to yellow-green fluorescence supports previous observations that the autofluorescent structures are lysosomes. A color shift from yellow-green (*A*) to yellow-red (*B*) is indicative of FTR accumulation in the same compartment. Small, discrete vesicles at the apical (arrows) and basal (arrowheads) membranes is indicative of early endosomes or transcytotic vesicles. Exposure to 10-fold excess folic acid (pH 7.0) 10 min before FTR infusion did not completely inhibit uptake or surface binding at the apical surface (*C* and *D*, asterisks). Endocytic vesicles were still seen at the apical (arrows) and basal (arrowheads) sides, although they appeared dimmer. The color shift seen in *A* and *B* is not as apparent in *C* and *D*. Bar = ~10 μm.

defects (21, 47), and increased risk of vascular disease due to hyperhomocysteinemia (6). Because of the importance of the kidneys in retention of folic acid from urinary excretion, the mechanism of folic acid recycling by kidney proximal tubules has been well studied (2, 3, 9, 10, 14, 22, 25, 32, 34–37, 41, 48, 50, 52). The fate of folate after kidney binding and uptake is also important because of the use of folic acid as a "Trojan horse" in targeting chemotherapeutics to tumors, which could potentially also cause toxicity to the kidney (30, 40). Until now, progress in characterizing folate salvage pathways in the kidney has been made mainly by using excised proximal tubules or kidney cells in culture with either protein gold conjugates linked to folate or radioactive folic acid (2, 3, 9, 10,

14, 22, 25, 32, 34–37, 41, 48, 50, 52, 54). By using these approaches, evidence for accumulation within large, discrete vesicles of the clathrin-coated-pit pathway has been reported (2–4).

While these studies are very illuminating, the previously available technology did not permit continuous observation of the pathway under in vivo physiological conditions. Because folate gold nanoparticles and anti-folate receptor antibodies are multivalent, and because multimerization of folate receptors by antibodies has been shown to affect the internalization itinerary (34), data from these studies may not reflect the intracellular pathway taken by monomeric folate conjugates after internalization (2, 3). Although studies with [^{3}H]folate uptake into
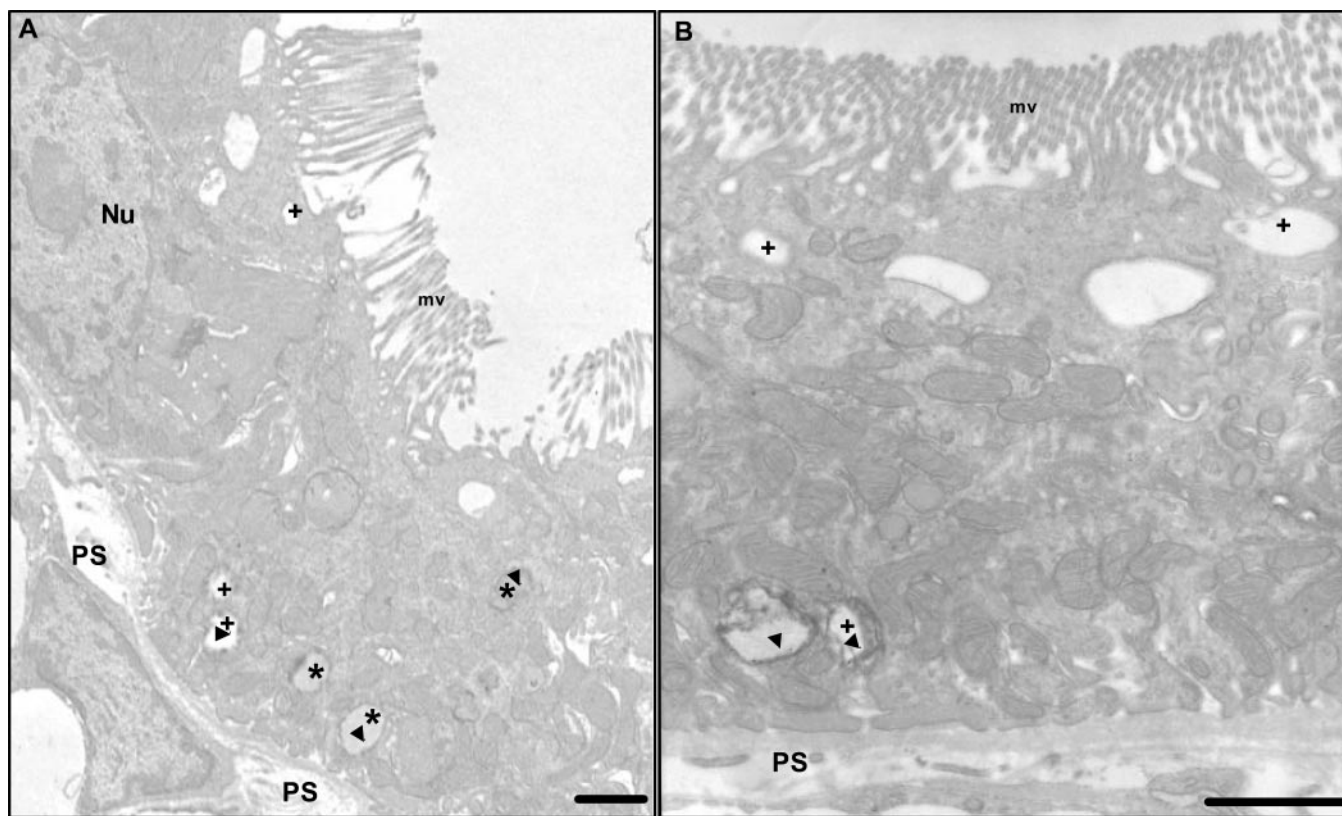
Fig. 6. Electron photomicrographs of FTR photoconverted in the presence of diaminobenzadine to yield an electron-dense reaction product for direct localization. Cross sections of proximal tubules with the characteristic microvasculature contain FTR reaction product localized within the membranes of vesicular structures (A and B, arrowheads). Within the interior of the cell, the reaction product is localized in more opaque, proteinaceous vesicles (asterisks). At the apical and basal membranes, less opaque vesicles with density matching the extracellular space (plus signs) are present. At the basal side, some of these vesicles also contain reaction product (arrowheads), indicating direct access to the basal lumen or peritubular space (PS). Nu, nucleus. Bars = ~1 μm.

kidney proximal tubules in vivo followed by radiography allow a more accurate assessment of the internalization pathway for folic acid (22), they do not allow continuous tracking of folic acid binding, endocytosis, and intracellular transport, which is possible with in vivo two-photon microscopy.

In the present study, several important aspects of intracellular folate handling are described. First, internalization occurs rapidly via endocytosis, with the bulk of the compound directed to the lysosomal pool. Second, strong evidence from electron and fluorescence microscopic data supports a mechanism for transcytosis directly from the apical to the basal membrane. Accumulation of FTR-containing vesicles at the subapical region without subsequent migration to the basal pole after colchicine treatment further supports evidence for transcytosis. Although vesicles derived from both clathrin-coated pits and caveolae use microtubules for intracellular movement, the lack of caveolin expression at the apical surface of proximal tubules (7) suggests that this phenomenon occurs via the former.

Lack of colocalization between dextrans and FTR in these discrete basal vesicles suggests that they did not originate from lysosomes. Also, during the initial infusion of FTR, movement into the peritubular space was seen. FTR quickly returned to the plasma volume, because no trace of residual FTR was seen in these areas after 4 min. The appearance of the small basal vesicles occurred too long after FTR infusion to be accounted

for by the transient phenomenon of leakage into the peritubular space.

During these experiments, at no time was there evidence of FTR freely released into the cytosol of proximal tubule cells. Previous publications have noted this with the use of radiolabeled forms of folate when different cellular fractions were examined (22). When using such procedures, the risk of rupturing compartments containing the marker and contaminating other fractions raises concerns. Lack of cytosolic localization further bolsters the observation that internalization occurs solely though endocytosis and not likely through a surface channel. One limitation of this study is the inability to attain quantitative information, particularly for the fraction that is transcytosed. Continued accumulation of FTR within the lysosomes quickly creates a highly fluorescent intracellular compartment. Vesicles destined for transcytosis near the basal membranes conversely remain relatively dim. In addition, defining a transcytotic vesicle simply by close proximity to the basal membrane presents another pitfall that could lead to an overestimation, because not all vesicles at the basal pole will fuse. Finally, once transcytosis occurs, the dim, compartmentalized fluorescence is immediately lost as the contents are diluted with fluid in the peritubular space. Studies in which [³H]folate was used in isolated, microperfused rabbit proximal tubules reported transcytosis of ~5% of the perfused amount (2). Barring species differences between rabbit and rat, this

established value would likely be similar because those studies also used an intact tubule.

In conclusion, this study exploits newly developed techniques in live animal imaging to study the fate of a fluorescent analog of folate after internalization by proximal tubule cells. Taking our present results together with previous data, we surmise that the bulk of folate endocytosed by the cells trafficks directly to the lysosomes, where it is retained, while the receptor recycles back to the surface membrane. A small pool of folate is transcytosed directly across the cell to the basal membrane, with no evidence of cytosolic distribution throughout the length of the study. This result is contraindicative of the fate of folate in neoplastic cells, where cytosolic release in tumor cells is readily observed (40, 54). This underlying difference may play a pivotal role in the toxicity of folate drug conjugates to tumor cells and the absence of toxicity of the same conjugates to the kidney.

REFERENCES

1. **Anderson RG, Kamen BA, Rothberg KG, and Lacey SW.** Potocytosis: sequestration and transport of small molecules by caveolae. *Science* 255: 410–411, 1992.
2. **Birn H, Nielsen S, and Christensen EI.** Internalization and apical-to-basolateral transport of folate in rat kidney proximal tubule. *Am J Physiol Renal Physiol* 272: F70–F78, 1997.
3. **Birn H, Selhub J, and Christensen EI.** Internalization and intracellular transport of folate-binding protein in rat kidney proximal tubule. *Am J Physiol Cell Physiol* 264: C302–C310, 1993.
4. **Botez MI.** Folate deficiency and neurological disorders in adults. *Med Hypotheses* 2: 135–140, 1976.
5. **Bottiglieri T, Hyland K, Laundy M, Godfrey P, Carney MW, Toone BK, and Reynolds EH.** Folate deficiency, biopterin and monoamine metabolism in depression. *Psychol Med* 22: 871–876, 1992.
6. **Boushey CJ, Beresford SA, Omenn GS, and Motulsky AG.** A quantitative assessment of plasma homocysteine as a risk factor for vascular disease. Probable benefits of increasing folic acid intakes. *JAMA* 274: 1049–1057, 1995.
7. **Breton S, Lisanti MP, Tyszkowski R, McLaughlin M, and Brown D.** Basolateral distribution of caveolin-1 in the kidney: absence from H^+-ATPase-coated endocytic vesicles in intercalated cells. *J Histochem Cytochem* 46: 205–214, 1998.
8. **Chang WJ, Rothberg KG, Kamen BA, and Anderson RG.** Lowering the cholesterol content of MA104 cells inhibits receptor-mediated transport of folate. *J Cell Biol* 118: 63–69, 1992.
9. **Chatterjee S, Smith ER, Hanada K, Stevens VL, and Mayor S.** GPI anchoring leads to sphingolipid-dependent retention of endocytosed proteins in the recycling endosomal compartment. *EMBO J* 20: 1583–1592, 2001.
10. **Christensen EI, Birn H, Verroust P, and Moestrup SK.** Membrane receptors for endocytosis in the renal proximal tubule. *Int Rev Cytol* 180: 237–284, 1998.
11. **Cooperman JM, Pesci-Bourel A, and Luhby AL.** Urinary excretion of folic acid activity in man. *Clin Chem* 16: 375–381, 1970.
12. **Corrocher R, Abramson RG, King VF, Schreiber C, Dikman S, and Waxman S.** Differential binding of folates by rat renal cortex brush border and basolateral membrane preparations. *Proc Soc Exp Biol Med* 178: 73–84, 1985.
13. **Dunn KW, Sandoval RM, Kelly KJ, Dagher PC, Tanner GA, Atkinson SJ, Bacallao RL, and Molitoris BA.** Functional studies of the kidney of living animals using multicolor two-photon microscopy. *Am J Physiol Cell Physiol* 283: C905–C916, 2002.
14. **Fan J, Kureshy N, Vitols KS, and Huennekens FM.** Novel substrate analogs delineate an endocytic mechanism for uptake of folate via the high-affinity, glycosylphosphatidylinositol-linked transport protein in L1210 mouse leukemia cells. *Oncol Res* 7: 511–516, 1995.
15. **Fernandes-Costa F and Metz J.** Binding of methylfolate and pteroylglutamic acid by the specific serum folate binder. *J Lab Clin Med* 93: 181–188, 1979.
16. **Forshaw J and Harwood L.** Diagnostic value of the serum folate assay. *J Clin Pathol* 24: 244–249, 1971.
17. **Futter CE, Pearse A, Hewlett LJ, and Hopkins CR.** Multivesicular endosomes containing internalized EGF-EGF receptor complexes mature and then fuse directly with lysosomes. *J Cell Biol* 132: 1011–1023, 1996.
18. **Golnik KC and Newman SA.** Anterior ischemic optic neuropathy associated with macrocytic anemia. *J Clin Neuroophthalmol* 10: 244–247, 1990.
19. **Golnik KC and Schaible ER.** Folate-responsive optic neuropathy. *J Neuroophthalmol* 14: 163–169, 1994.
20. **Herbert V.** Anemias. *Curr Concepts Nutr* 5: 79–89, 1977.
21. **Hibbard ED and Smithells RW.** Folic acid metabolism and human embryopathy (Abstract). *Lancet* 285: 1254, 1965.
22. **Hjelle JT, Christensen EI, Carone FA, and Selhub J.** Cell fractionation and electron microscope studies of kidney folate-binding protein. *Am J Physiol Cell Physiol* 260: C338–C346, 1991.
23. **Hoffbrand AV and Herbert V.** Nutritional anemias. *Semin Hematol* 36: 13–23, 1999.
24. **Holm J, Hansen SI, Hoier-Madsen M, and Bostad L.** A high-affinity folate binding protein in proximal tubule cells of human kidney. *Kidney Int* 41: 50–55, 1992.
25. **Jansen G.** Receptor-and carrier-mediated transport systems for folates and antifolates: exploitation for folate-based chemotherapy and immunotherapy. In: *Cancer Drug Discovery and Development: Antifolate Drugs in Cancer Therapy*, edited by Jackman AL. Totowa, NJ: Humana, 1999, vol. 4, p. 293–321.
26. **Kamen BA and Caston JD.** Direct radiochemical assay for serum folate: competition between ^{3}H-folic acid and 5-methyltetrahydrofolic acid for a folate binder. *J Lab Clin Med* 83: 164–174, 1974.
27. **Kamen BA and Caston JD.** Identification of a folate binder in hog kidney. *J Biol Chem* 250: 2203–2205, 1975.
28. **Kennedy MD, Jallad KN, Lu J, Low PS, and Ben-Amotz D.** Evaluation of folate conjugate uptake and transport by the choroid plexus of mice. *Pharm Res* 20: 714–719, 2003.
29. **Knox DL, Chen MF, Guilarte TR, Dang CV, and Burnette J.** Nutritional amblyopia: folic acid, vitamin B-12, and other vitamins. *Retina* 2: 288–293, 1982.
30. **Leamon CP and Low PS.** Folate-mediated targeting: from diagnostics to drug and gene delivery. *Drug Discov Today* 6: 44–51, 2001.
31. **Luo J, Smith MD, Lantrip DA, Wang S, and Fuchs PL.** Efficient syntheses of pyrofolic acid and pteroyl azide, reagents for the production of carboxyl-differentiated derivatives of folic acid. *J Am Chem Soc* 119: 10004–10013, 1997.
32. **Masereeuw R, Russel FG, and Miller DS.** Multiple pathways of organic anion secretion in renal proximal tubule revealed by confocal microscopy. *Am J Physiol Renal Fluid Electrolyte Physiol* 271: F1173–F1182, 1996.
33. **Matherly LH and Goldman DI.** Membrane transport of folates. *Vitam Horm* 66: 403–456, 2003.
34. **Mayor S, Rothberg KG, and Maxfield FR.** Sequestration of GPI-anchored proteins in caveolae triggered by cross-linking. *Science* 264: 1948–1951, 1994.
35. **Mayor S, Sabharanjak S, and Maxfield FR.** Cholesterol-dependent retention of GPI-anchored proteins in endosomes. *EMBO J* 17: 4626–4638, 1998.
36. **McMartin KE, Eisenga BH, and Collins TD.** Renal uptake and metabolism of 5-methyltetrahydrofolate in the rat. In: *Chemistry and Biology of Pteridines, 1989: Pteridines and Folic Acid Derivatives: Proceedings of the 9th International Symposium on Pteridines and Folic Acid Derivatives*, edited by Ghisla S, Blau N, and Curtius HC. Berlin: de Gruyter, 1990, p. 1276–1279.
37. **McMartin KE, Morshed KM, Hazen-Martin DJ, and Sens DA.** Folate transport and binding by cultured human proximal tubule cells. *Am J Physiol Renal Fluid Electrolyte Physiol* 263: F841–F848, 1992.
38. **Morris MS, Fava M, Jacques PF, Selhub J, and Rosenberg IH.** Depression and folate status in the US population. *Psychother Psychosom* 72: 80–87, 2003.
39. **Odorizzi G, Pearse A, Domingo D, Trowbridge IS, and Hopkins CR.** Apical and basolateral endosomes of MDCK cells are interconnected and contain a polarized sorting mechanism. *J Cell Biol* 135: 139–152, 1996.

40. **Reddy JA and Low PS.** Folate-mediated targeting of therapeutic and imaging agents to cancers. *Crit Rev Ther Drug Carrier Syst* 15: 587–627, 1998.

41. **Rijnboutt S, Jansen G, Posthuma G, Hynes JB, Schornagel JH, and Strous GJ.** Endocytosis of GPI-linked membrane folate receptor-α. *J Cell Biol* 132: 35–47, 1996.

42. **Ritter TE, Fajardo O, Matsue H, Anderson RG, and Lacey SW.** Folate receptors targeted to clathrin-coated pits cannot regulate vitamin uptake. *Proc Natl Acad Sci USA* 92: 3824–3828, 1995.

43. **Rothberg KG, Ying YS, Kolhouse JF, Kamen BA, and Anderson RG.** The glycophospholipid-linked folate receptor internalizes folate without entering the clathrin-coated pit endocytic pathway. *J Cell Biol* 110: 637–649, 1990.

44. **Sabolic I, Herak-Kramberger CM, Ljubojevic M, Biemesderfer D, and Brown D.** NHE3 and NHERF are targeted to the basolateral membrane in proximal tubules of colchicine-treated rats. *Kidney Int* 61: 1351–1364, 2002.

45. **Sandell JH and Masland RH.** Photoconversion of some fluorescent markers to a diaminobenzidine product. *J Histochem Cytochem* 36: 555–559, 1988.

46. **Sandoval R, Leiser J, and Molitoris BA.** Aminoglycoside antibiotics traffic to the Golgi complex in LLC-PK1 cells. *J Am Soc Nephrol* 9: 167–174, 1998.

47. **Scott JM, Weir DG, and Kirke PN.** Folate and neural tube defects. *Clin Nutr Health Dis* 1: 329–360, 1995.

48. **Selhub J, Emmanouel D, Stavropoulos T, and Arnold R.** Renal folate absorption and the kidney folate binding protein: I. Urinary clearance studies. *Am J Physiol Renal Fluid Electrolyte Physiol* 252: F750–F756, 1987.

49. **Selhub J and Franklin WA.** The folate-binding protein of rat kidney. Purification, properties, and cellular distribution. *J Biol Chem* 259: 6601–6606, 1984.

50. **Selhub J, Nakamura S, and Carone FA.** Renal folate absorption and the kidney folate binding protein: II. Microinfusion studies. *Am J Physiol Renal Fluid Electrolyte Physiol* 252: F757–F760, 1987.

51. **Selhub J and Rosenberg IH.** Demonstration of high-affinity folate binding activity associated with the brush border membranes of rat kidney. *Proc Natl Acad Sci USA* 75: 3090–3093, 1978.

52. **Sikka PK and McMartin KE.** Determination of folate transport pathways in cultured rat proximal tubule cells. *Chem Biol Interact* 114: 15–31, 1998.

53. **Sundin DP, Sandoval R, and Molitoris BA.** Gentamicin inhibits renal protein and phospholipid metabolism in rats: implications involving intracellular trafficking. *J Am Soc Nephrol* 12: 114–123, 2001.

54. **Turek JJ, Leamon CP, and Low PS.** Endocytosis of folate-protein conjugates: ultrastructural localization in KB cells. *J Cell Sci* 106: 423–430, 1993.

55. **Wang Y, Zhao R, Russell RG, and Goldman ID.** Localization of the murine reduced folate carrier as assessed by immunohistochemical analysis. *Biochim Biophys Acta* 1513: 49–54, 2001.

56. **Winick NJ, Bowman WP, Kamen BA, Roach ES, Rollins N, Jacaruso D, and Buchanan GR.** Unexpected acute neurologic toxicity in the treatment of children with acute lymphoblastic leukemia. *J Natl Cancer Inst* 84: 252–256, 1992.